Fronts in a bistable medium with two global constraints: Oscillatory instability and large-amplitude limit-cycle motion

M. Meixner, P. Rodin,* and E. Schöll
Institut für Theoretische Physik, Technische Universität Berlin, Hardenbergstraße 36, D-10623 Berlin, Germany
(Received 22 June 1998)

We study the propagation of fronts in a reaction-diffusion model of a bistable medium with two global constraints. The model applies to lateral current density fronts in three-electrode bistable semiconductor systems driven by the main and gate circuits. When taken separately, these constraints provide positive and negative feedbacks on front dynamics leading to accelerated and decelerated fronts, respectively. Under two constraints, there is an interplay between positive and negative feedback resulting in an oscillatory instability of a stationary front and large-amplitude limit-cycle motion. The instability occurs purely due to the global coupling and is not sensitive to the effect of the boundaries. [S1063-651X(98)12311-5]

PACS number(s): 05.70.Ln, 72.20.Ht, 85.30.−z

I. INTRODUCTION AND MODEL

Global and nonlocal coupling has been recently recognized as an important factor for pattern formation in spatially extended active media [1–11]. Generally, global coupling is related to external constraints imposed on the system dynamics. For lateral current density patterns in bistable semiconductor systems the global coupling is introduced by the external circuit which is used for operating the system [12]. In such systems the global excitation level can be characterized by the voltage applied across the device. The dynamics of a self-organized nonlinear pattern (e.g., current filament, lateral current density front, etc.) that causes a variation of the total current simultaneously changes the voltage drop at the external load and/or internal resistance of the voltage source. That leads to the variation of the voltage across the device. This type of feedback is well known with respect to stationary [12,13] and spiking filaments [14] in bistable semiconductor elements and has been recently discussed for lateral current density fronts [15].

In this paper we introduce a model of a bistable medium with *two* global constraints. The model applies to lateral current density fronts in three-electrode (gate-driven) bistable semiconductor *pnpn* structures (Fig. 1). If such a structure is switched from the low conductivity to the high conductivity state, a switching front triggers double injection of electrons and holes from cathode and anode increasing the concentration of excess carriers up to ten orders of magnitude. The resulting dramatic increase of both conductivity and light emission provides a basis for numerous applications not only in power electronics and optoelectronics [16] but also in pattern recognition [17,18]. Generally, the spatiotemporal dynamics of current density distributions in a gate-driven structure should be considered together with *two* global constraints imposed on the internal dynamics by the external main and gate circuits [19]. Recently we have shown that the type of feedback upon the front dynamics provided by constraints via the main and gate circuits, respectively, is qualitatively different [15]: Whereas for the gate circuit the feedback is positive (*activatory constraint*) and results in acceleration of the front motion [15], for the main circuit it is negative (*inhibitory constraint*) and leads to deceleration (see also [13]). In this article we study the complex dynamics of current density fronts that occur due to the interplay between negative and positive feedbacks. We demonstrate that the destabilizing action of the activatory constraint together with the stabilizing effect of the inhibitory constraint may result in an *oscillatory instability* of a stationary front and large-amplitude *limit-cycle motion*. In contrast to bistable systems

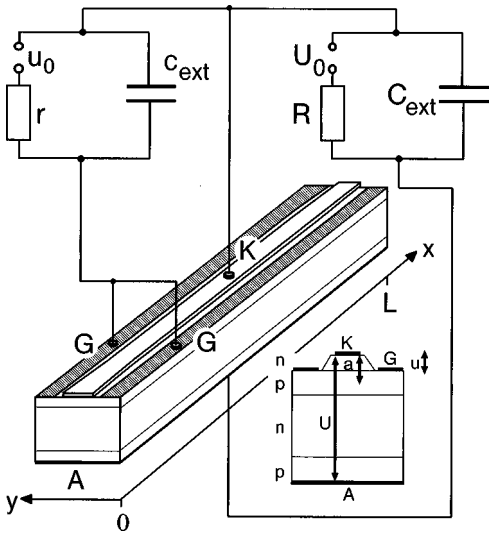

FIG. 1. Sketch of the gate-driven *pnpn* structure and the external circuits. The potential drops between the cathode *K* and the *p* layer, the gate *G*, and the anode *A* are denoted by *a*, *u*, and *U*, respectively. The variable *a* controls the internal state of the device. High values of *a* correspond to the high conductivity state of the device and high current density *J* between the cathode and anode. The current density front propagates in the transverse direction along the *x* axis. The spatial distribution of *a* along the *y* axis is assumed to be homogeneous. The inset shows the cross section of the structure.

*On leave from A. F. Ioffe Physicotechnical Institute, Russian Academy of Science, 194021 St. Petersburg, Russia. Electronic address: pavel@rodin.ioffe.rssi.ru

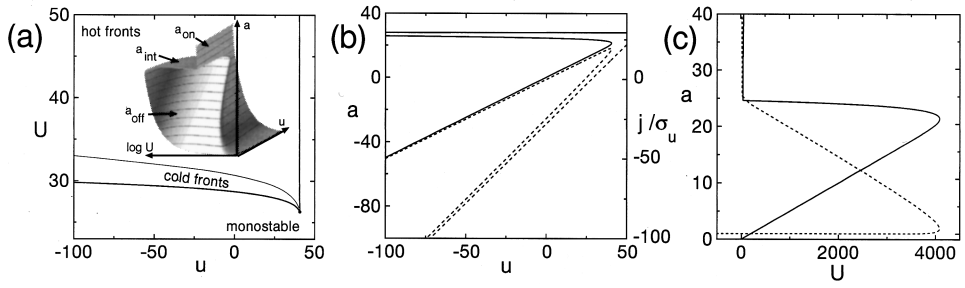

FIG. 2. Bistable and monostable regimes of the active medium. (a) Different regimes in the plane of control voltage u and supply voltage U. For the monostable regime the $a(u,U)$ dependence is single valued. For the bistable regime there are two values $a_{\rm on}$, $a_{\rm off}$ corresponding to the stable homogeneous on and off states, respectively, and an intermediate unstable state $a_{\rm int}$. The inset shows the homogeneous stationary $a(u,U)$ dependence. Regimes related to hot fronts ($a_{\rm on}$ propagates into $a_{\rm off}$) and cold fronts ($a_{\rm off}$ propagates into $a_{\rm on}$) are depicted. The line separating these two regimes corresponds to zero front velocity $v(u,U)=0$. (b),(c) Cross sections $a(u)$ and $a(U)$ of the $a(u,U)$ dependence at $U=30.75$ and $u=0$, respectively. The point $u=0$, $U=30.75$ corresponds to a stationary front. The dashed lines show the corresponding current-voltage characteristics $j(u)\equiv j(a(u),u)$ and $J(U)\equiv J(a(U),U)$ which are Z shaped for the gate circuit (b) and S shaped for the main circuit (c). The Ohmic component of the current density J is neglected. Here and throughout the paper the coefficients of the local kinetic functions $f(a,u,U)$ are chosen as $\alpha=2\times10^9$, $\beta=14.5$, $\gamma=10^7$, $\kappa=10^9$ as in [15]. All potentials a, u, U, and j/σ_u are in units of kT/e; J is in units of J_S.

with a single global constraint, where an oscillatory instability is caused by the attraction of a front by the system boundaries [13,15], under two constraints the instability occurs purely due to the global coupling and *is not* sensitive to the boundary conditions. Our consideration is applicable to any bistable medium with two global parameters controlling the front behavior.

The model equations

$$\tau_a\frac{\partial a(x,t)}{\partial t}=l^2\frac{\partial^2 a(x,t)}{\partial x^2}+f(a,u,U),$$

$$x\in[0,L],\quad \left.\frac{\partial a}{\partial x}\right|_{0,L}=0, \tag{1}$$

$$\tau_u(u)\frac{du}{dt}=u_0-u-r\int_0^L j(a,u)dx,\quad \tau_u(u)\equiv rc(u),$$

$$c(u)\equiv c_{\rm ext}+c_{\rm int}, \tag{2}$$

$$\tau_U(U)\frac{dU}{dt}=U_0-U-R\int_0^L J(a,u)dx,$$

$$\tau_U(U)\equiv RC(U),\quad C(U)\equiv C_{\rm ext}+C_{\rm int} \tag{3}$$

describe a gate-driven multilayer semiconductor structure [19,15] as shown in Fig. 1. The internal state of the structure is characterized by the order parameter $a(x,t)$ determining the bistability and is governed by the reaction-diffusion equation (1) with a nonpolynomial local kinetic function [20,15]

$$f(a,u,U)\equiv-\alpha a+\exp a-\beta\exp(-U+2a)+\gamma U+\kappa u. \tag{4}$$

The order parameter a has the meaning of the p-base potential. The characteristic length l and the coefficients α, β, γ, κ of the local kinetic function are determined by the structural parameters [20], τ_a is the characteristic relaxation time of a (see [15,20] for details). Neumann boundary conditions for $a(x,t)$ are assumed. Cathode-gate and cathode-anode voltages are denoted by u and U, respectively. All potentials a, u, U are in units of kT/e. The dynamics of u and U is described by Kirchhoff's equations (2), (3) for the main and control circuit, respectively (Fig. 1). For the current density per unit length between the gate and the cathode $j(a,u)$, and between the cathode and anode $J(a,U)$ we assume [19,15]

$$J(a,U)=\sigma_U U+J_S(\exp a-1),\quad j(a,u)=\sigma_u(u-a), \tag{5}$$

with linear conductivities σ_U, σ_u. Equations (2) and (3) represent global constraints imposed on the internal dynamics of $a(x,t)$ and have the form of dynamical equations for the variables u, U of the bistable medium. The limit case of two static constraints $\tau_u,\tau_U=0$ has been studied in [19]. Hereinafter capital and small letters refer to the main and gate circuits, respectively. The characteristic relaxation times $\tau_u(u),\tau_U(U)$ are determined by the sums of the differential capacitances of the external circuits $c_{\rm ext}$, $C_{\rm ext}$ and the differential cathode-gate and cathode-anode capacitances $c_{\rm int}$, $C_{\rm int}$, respectively. Null isoclines related to these constraints are controlled by the external loads $r>0$, $R>0$ and the voltage sources u_0, U_0.

The $a(u,U)$ dependence that results from the null isocline $f(a,u,U)=0$ is bistable in a certain range of parameters u, U [Fig. 2(a)]. The $a(u)$ dependence calculated for $U=$const [Fig. 2(b)] and the $a(U)$ dependence calculated for $u=$const [Fig. 2(c)] are both S shaped. The local current-voltage characteristic related to the gate circuit $j(u)\equiv j(a(u),u)$ is Z shaped [Fig. 2(b)] and the local current-voltage characteristic related to the main circuit $J(U)\equiv J(a(U),U)$ is S shaped [Fig. 2(c)]. For $u,U=$const corresponding to the bistable regime any steplike initial profile $a(x)$ which consists of the two stable homogeneous steady states $a_{\rm on}$ and $a_{\rm off}$ [see Fig. 2(a)] develops into a moving front which propagates in a self-similar way with a constant velocity $v(u,U)$ (Fig. 3). This corresponds to the propaga-

tion of a stable state into a metastable state [21]. The direction of the front propagation is determined by the sign of the integral [22]

$$A(u,U)\equiv\int_{a_{\rm off}}^{a_{\rm on}} f(a,u,U)da. \tag{6}$$

For $A>0$ the on state propagates into the off state ($v>0$, *hot front*) and for $A<0$ the off state propagates into the on state ($v<0$, *cold front*). The line of zero velocity $v(u,U)=0$ corresponds to the parameters u_{co},U_{co} given by the equal areas rule $A(u_{co},U_{co})=0$ [12,22], where co stands for phase coexistence. Note that this line, separating hot and cold fronts, is also shown in Fig. 2(a). In sufficiently large systems ($L\gg W$, where W is a characteristic front width) the relaxation of the homogeneous plateaus of the kink pattern is faster than the motion of the front wall and therefore the velocity of the globally coupled front is determined by the instantaneous values of the global parameters u and U with good accuracy [1,15].

II. POSITIVE AND NEGATIVE FEEDBACKS UPON FRONT DYNAMICS: ACCELERATED AND DECELERATED FRONTS

First let us discuss the action of the global constraints on front dynamics separately for $U=$const and for $u=$const. Consider the propagation of a hot front for $U=$const when global coupling occurs only via the constraint (2). Since $\partial j/\partial a<0$, the total current in the control circuit decreases as the front propagates and therefore u increases. Due to $\partial v/\partial u>0$ (Fig. 3) that leads to accelerated motion. For a cold front u decreases which also leads to an increase of the absolute value of the front velocity. So we conclude that the global constraint (2) provides positive feedback upon the front dynamics. Any stationary front is destabilized by this feedback and starts to move towards the boundary. For $r>0$ these conclusions hold generally for systems with Z-shaped current-voltage characteristics (see [15] for a detailed analysis of this case). For $u=$const, when the global coupling occurs only via the constraint (3), we take into account that $\partial J/\partial a>0$, $\partial v/\partial U>0$. Then a similar reasoning shows that the front propagation is accompanied by a decrease or an increase of U for hot or cold fronts, respectively. That implies negative feedback upon the front dynamics as it generally occurs for semiconductor systems with S-shaped current-voltage characteristics. Propagation of a hot decelerated front can lead the system to the homogeneous on state or to a stationary kink pattern. The last situation takes place if U reaches the value U_{co} determined by $A=0$. This kink pattern is stable for sufficiently large R (regime of strong global coupling) and small τ_U (fast response of the inhibitory global constraint) [13].

So we conclude that a propagating front experiences positive and negative feedback via the main and control circuits, respectively. Since these feedbacks are most efficient for large values of r, R [13,15] in the following we assume current-controlled conditions in both circuits: $r,R\to\infty$, $u_0/r\to i_0$, $U_0/R\to I_0$, where i_0 and I_0 are the total currents in the gate and main circuits, respectively. We also assume that t and x are measured in units of τ_a and l ($t\to t/\tau_a$, $x\to x/l$), respectively. Then Eqs. (1)–(3) take the dimensionless form:

$$\frac{\partial a}{\partial t}=\frac{\partial^2 a}{\partial x^2}+f(a,u,U), \tag{7}$$

$$\epsilon\frac{du}{dt}=j_0-u+\langle a\rangle,\quad \epsilon\equiv\frac{c}{\tau_a\sigma_u L},\quad j_0\equiv\frac{i_0}{\sigma_u L}, \tag{8}$$

$$\xi\frac{dU}{dt}=J_0-\langle\exp a-1\rangle,\quad \xi\equiv\frac{C}{\tau_a J_S L},\quad J_0\equiv\frac{I_0}{J_S L}, \tag{9}$$

where angular brackets denote the spatial average over the system length L. Here we have neglected the Ohmic component $\sigma_U U$ of the current density J [see Eq. (5)]. The parameters ϵ and ξ, which have substituted τ_u and τ_U, respectively, characterize the relaxation times related to the global constraints and determine the delay of the feedback upon the front dynamics provided by these constraints. This feedback is instantaneous and hence most efficient for $\epsilon,\xi\to 0$ and vanishes for $\epsilon,\xi\to\infty$.

III. OSCILLATORY REGIMES OF FRONT DYNAMICS UNDER TWO CONSTRAINTS

Now we shall study front propagation in the presence of two constraints. Consider a stationary solution $a_0(x),U_{co},u_{co}$ of Eqs. (7)–(9) that corresponds to the steady front located in the center of the system at $x_0=L/2$ (inset of Fig. 4). The stability of this pattern has been studied numerically for a wide range of parameters ϵ, ξ (Fig. 4). The boundary between stable and unstable regimes in the (ϵ, ξ) plane corresponds to an oscillatory instability. (The saddle-type instabilities that may occur in this model have been studied for $\epsilon=0$, $\xi=0$ in [19].) The oscillation frequency $\nu\sim\xi^{-0.5}$ at the bifurcation point is given by the relaxation time ξ in the main circuit (Fig. 4, dotted line). It is readily seen that the dynamics can be tuned by adjusting ϵ and ξ. Let us discuss the results of the stability analysis for the limit cases of slow and fast relaxation.

For $\epsilon\to\infty$, $\xi\to\infty$ both global parameters u, U do not respond to front position and keep their initial values $u=u_0$, $U=U_0$. Therefore the front dynamics is free from global

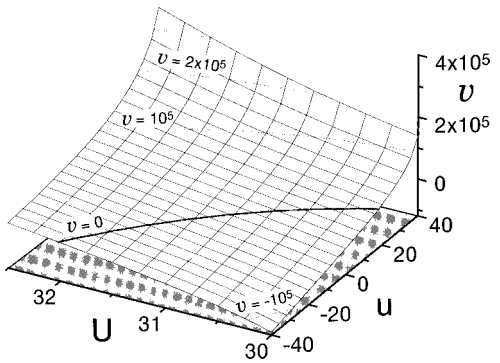

FIG. 3. Front velocity v as a function of the parameters u, U obtained by direct numercal simulations. Positive and negative velocities correspond to hot and cold fronts, respectively. The front velocity v is in units of l/τ_a, u and U are in units of kT/e.

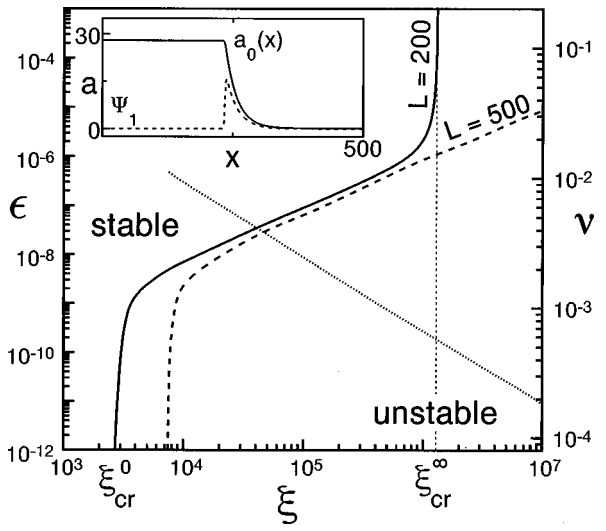

FIG. 4. Regimes of stability of the stationary front $a_0(x)$ located at $x_0=L/2$ for $u_0=0$, $U_0=30.75$ (see inset) in the plane of the time scales of the global constraints (ϵ,ξ). The boundary between stable and unstable regimes corresponds to the oscillatory instability. The simulations have been performed for $L=200$ (solid line) and $L=500$ (dashed line). Further simulations have shown that an increase of the system size beyond $L=500$ does not change the boundary between stable and unstable fronts. $\xi_{\rm cr}^0$, $\xi_{\rm cr}^\infty$ correspond to the limit cases $\epsilon\to 0$ and $\epsilon\to\infty$, respectively. The dotted line shows the oscillation frequency ν at the bifurcation point for $L=500$. Numerical parameters are $j_0=14.4$ and $J_0=6.99\times 10^{11}$; x and L are in units of l, ν is in units of $1/\tau_a$, a is in units of kT/e.

constraints in this case. The eigenmodes Ψ_i of the stationary kink solution $a_0(x)$ are determined by the Sturm-Liouville operator

$$H=\frac{d^2}{dx^2}+\left.\frac{\partial f}{\partial a}\right|_{a_0(x),u_0,U_0}, \tag{10}$$

which results from the linearization of Eq. (7) in the vicinity of $a_0(x)$. The first eigenmode $\Psi_1(x)$ corresponds to the translation of the front. In an infinite system its eigenvalue λ_1 is equal to zero due to the translation invariance: a stationary front has neutral stability. In a finite system λ_1 becomes positive reflecting the attractive action of the boundaries but decreases exponentially with the system size L [13]. For $\epsilon\to\infty$ [no positive feedback via Eq. (8)] but arbitrary ξ we have $u=u_0$ and Eq. (7) should be considered together with the inhibitory constraint (9). Negative feedback provided by Eq. (9) suppresses the unstable mode Ψ_1 as long as the response of the global constraint is sufficiently fast [13]. Increase of ξ eventually leads to the situation where ξ becomes larger than the increment λ_1^{-1} of the unstable translation mode Ψ_1 and therefore the global constraint cannot suppress this mode anymore. That causes an oscillatory instability of the stationary front occurring at $\xi=\xi_{\rm cr}^\infty$. Since for $\epsilon\to\infty$ positiveness of λ_1 purely results from the interaction of the front with a boundary, the oscillatory instability in this case essentially represents *a boundary effect* [13,15]. Due to the exponential decrease of λ_1 with increasing L in practice the oscillatory instability cannot be detected at all in sufficiently large systems. In our numerical simulations performed for two system sizes $L=200$ and $L=500$ (recall that L is in units of l) the critical value $\xi_{\rm cr}^\infty$ has been achieved only for the smaller system size $L=200$ (Fig. 4, solid line), since the instability occurs at very low frequency $\nu\sim(\xi_{\rm cr}^\infty)^{-0.5}$.

In the opposite limit case $\epsilon\to 0$ the positive feedback via the global constraint (8) is instantaneous. Eliminating u adiabatically, we combine Eqs. (7) and (8) into a single integro-differential equation

$$\frac{\partial a}{\partial t}=\frac{\partial^2 a}{\partial x^2}+f(a,j_0,U)+\kappa\langle a\rangle. \tag{11}$$

The equations of motion are given by Eqs. (11) and (9) in this case. The case $\epsilon\to 0$ is equivalent to the case $\epsilon\to\infty$ when Eq. (7) is substituted by Eq. (11). The eigenmodes of the stationary solution $a_0(x)$ of Eq. (11) are determined by the operator

$$\tilde{H}\equiv\frac{d^2}{dx^2}+\left.\frac{\partial f}{\partial a}\right|_{a_0(x),u_0,U_0}+\kappa\langle\cdots\rangle. \tag{12}$$

The self-adjoint operator $\tilde{H}$ is a sum of the Sturm-Liouville operator H and an integral operator of unit rank. The spectra λ_i and $\tilde{\lambda}_i$ of the operators H and $\tilde{H}$, respectively, are discrete and intermittent [23], i.e., there is one eigenvalue of the operator H between any two eigenvalues of the operator $\tilde{H}$ such that $\tilde{\lambda}_{i+1}<\lambda_i<\tilde{\lambda}_i$. This general feature of self-adjoint operators is not based on a perturbation theory with respect to κ and holds for arbitrary values of κ [23]. Obviously, the action of the integral component of the operator $\tilde{H}$ is proportional to the mean value $\langle\Psi_i\rangle$ of the eigenfunction Ψ_i. Therefore it is most efficient for the ground eigenfunction Ψ_1 which is strictly positive in the interior of the interval $(0,L)$. The increase of $\tilde{\lambda}_1$ with respect to λ_1 occurs due to the nonlocal coupling reflected by the integral term of Eq. (11). This increase leads to a severe decrease of the critical value $\xi_{\rm cr}^0$ with respect to $\xi_{\rm cr}^\infty$ (Fig. 4). The oscillation frequency increases by many orders of magnitude. The instability now results from the destabilizing positive feedback via the gate circuit, but not from interaction of a front with a boundary as it is for $\epsilon\to\infty$. This is consistent with the observation that $\xi_{\rm cr}^0$ weakly depends on the system size (Fig. 4, solid and dashed lines).

Along the line $\xi=\infty$ the parameter U does not change and keeps its initial value $U=U_0$. In this situation the global coupling occurs only via the constraint (8) and the dynamics is described by Eqs. (7) and (8) at $U=U_0$. A stationary pattern is always destabilized by the positive feedback provided by this constraint. In contrast, for instantaneous negative feedback $\xi=0$ prevents the instability for any value of ϵ.

The interplay between positive and negative feedbacks occurs for $\xi\in[\xi_{\rm cr}^0,\ \xi_{\rm cr}^\infty]$ (Fig. 4). The boundary of the oscillatory instability is represented approximately by a straight line in the (ϵ,ξ) plane (Fig. 4). Note that this general feature of the model (1),(2),(3) does not depend on the particular functions $f(a,u,U)$, $J(a,U)$, and $j(a,u)$ chosen. Here a decrease of ϵ enhances the positive feedback via the global

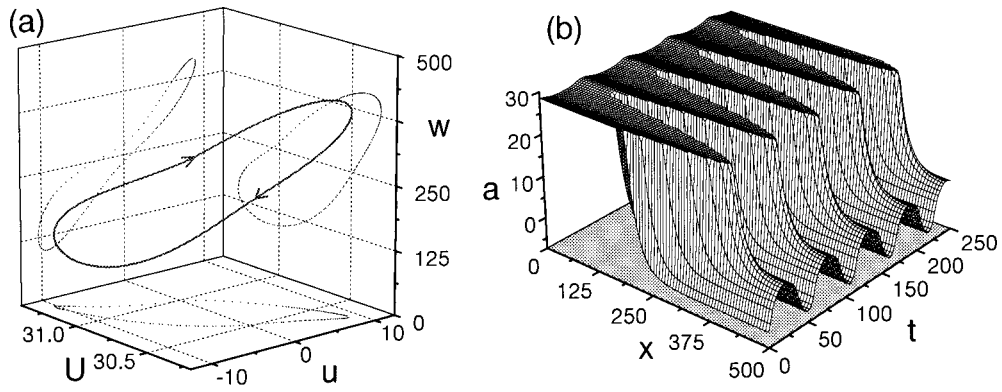

FIG. 5. Large amplitude limit-cycle oscillation of a front. (a) Phase portrait in the (w,u,U) space. The front position w is defined as the point x where $a(w,t)=0.5\times a_{\mathrm{on}}(t)$. Projections of the limit-cycle trajectory on the (w,u), (w,U), and (u,U) planes are shown as dotted lines. (b) Temporal evolution of $a(x,t)$ corresponding to the limit-cycle oscillation. Numerical simulations are performed for $L=500$, $\xi=10^4$, and $\epsilon=10^{-7}+10^{-8}\times u^2$, $j_0=14.4$, and $J_0=6.99\times 10^{11}$ as in Fig. 4; a, u, and U are in units of kT/e, w and x are in units of l, t is in units of τ_a.

constraint (8) and destabilizes the kink pattern whereas a decrease of ξ enhances the negative feedback via Eq. (9) and has a stabilizing effect. Therefore the stability of a stationary pattern as well as the oscillation frequency at the bifurcation point can be easily tuned by the parameters ϵ and ξ. However, for $\epsilon=$const, $\xi=$const the oscillations develop with increasing amplitude $A(t)\equiv w(t)-x_0$ [here $w(t)$ denotes the front position defined by $a(w,t)=0.5\times a_{\mathrm{on}}(t)$] and eventually at $A(t)=L/2$ the front reaches the boundary. Starting from this point the system remains in the homogeneous state exhibiting relaxation-type self-sustained oscillations.

Various mechanisms limiting the amplitude of front oscillations can be suggested. In particular, self-sustained limit-cycle oscillations with a fixed amplitude $A_0<L/2$ become possible if ϵ and/or ξ depend on the value of u and U, respectively. Indeed, growing oscillations of the front position are accompanied by growing oscillations of u and U around u_0 and U_0, respectively. Provided that $\epsilon(u)$ increases and $\xi(U)$ decreases with increase of $|u-u_0|$ and $|U-U_0|$, respectively, the positive feedback is diminished and the negative feedback is enhanced as the amplitude of the oscillations grows. These limiting mechanisms could act jointly if both ϵ and ξ depend on the corresponding voltages, or separately if one of these parameters remains constant. According to Eqs. (8) and (9) ϵ and ξ are proportional to the differential capacitances of the external circuits c_{ext} and C_{ext}, respectively. Therefore appropriate voltage dependencies can be introduced by nonlinear external capacitances. Recently active external circuits have been implemented for experimental studies of multistable systems [24] and discussed with respect to control over spatiotemporal dynamics [25,15]. In particular, negative capacitance and resistance have been realized in [24]. In the case under consideration, a simpler type of nonlinear capacitance suffices: it should be positive and substantially depend on the applied voltage. For instance, a steplike dependence of the differential capacitance providing $c(u)=c_1$ for $|u-u_0|<u_{\mathrm{th}}$ and $c(u)=c_2$ for $|u-u_0|>u_{\mathrm{th}}$ can be realized by an active circuit which effects switching between two different capacitances depending upon the voltage drop across the semiconductor element [26]; a decreasing dependence $\epsilon(U)$ of the external capacitance can be achieved by a varactor diode. In this paper we restrict ourselves to the case of an $\epsilon(u)$ dependence. We have performed simulations for a cubic nonlinearity of the external capacitance which results in a second order correction to the differential capacitance: $c_{\mathrm{ext}}(u)=c_0+c_1|u-u_0|^2$. The corresponding $\epsilon(u)$ dependence is then given by $\epsilon(u)=\epsilon_0+\epsilon_1|u-u_0|^2$. The values of ϵ_0 correspond to the unstable regime of ϵ in the (ϵ,ξ) plane and trigger the instability of the stationary front for u close to u_0. For a sufficiently large value of ϵ_1 the oscillations develop into a stable limit cycle corresponding to oscillations of the front position (Fig. 5). The amplitude of these self-sustained oscillations can be tuned by the parameters ϵ_0, ϵ_1 and may be increased up to $L/2$. The frequency can be tuned by the parameter ξ. Generally, the limit-cycle motion is not sensitive to a particular type of $\epsilon(u)$ dependence and may occur for any value of ξ from the interval $[\xi_{\mathrm{cr}}^0,\xi_{\mathrm{cr}}^\infty]$.

We propose that the amplitude of the oscillations might also be limited by implementing a second order resonance external circuit that includes an inductance as well, or by imposing asymmetric boundary conditions $a(0,t)=a_{\mathrm{on}}(u_0,U_0)$, $a(L,t)=a_{\mathrm{off}}(u_0,U_0)$ that keep the front off the boundary and can be implemented by additional lateral gates (see [15]).

IV. CONCLUSION

In conclusion, we have proposed a mechanism of an oscillatory instability and large-amplitude limit cycle motion of a front in a bistable medium. The mechanism is based on imposing two global constraints that provide positive *and* negative feedback upon the front dynamics and act with adjustable delay. When taken separately, these constraints result in propagation of accelerated and decelerated fronts, respectively. Under two constraints, there is an interplay between feedbacks of different types: Destabilizing action of the positive feedback together with the suppressing action of negative feedback leads to an oscillatory behavior of the front. The frequency of these oscillations is controlled by the relaxation time of the inhibitory constraint. The instability mechanism occurs purely due to the global coupling and is

not sensitive to the boundary conditions. Limit-cycle oscillations become possible if the relaxation time of one or both global constraints depends on the respective global parameter of the bistable medium. For appropriate parameters self-sustained oscillations can spread over almost the whole system (Fig. 5). For a *pnpn* structure considered here large-amplitude self-sustained oscillations correspond to the periodic spreading and shrinking of a highly modulated area of a dense electron-hole plasma with an amplitude and frequency easily controlled by external circuits. For light emitting and laser GaAs structures this amounts to an oscillation of the active area, which lends itself to applications in optical systems. However, the suggested mechanism is rather general and may occur in other bistable media with two global parameters controlling the front behavior as well. In particular, we note chemical reaction systems where global coupling may be light induced [7] as well as imposed via the gas phase [8], and bistable electrochemical systems [10] where global and nonlocal coupling via the external circuit and the electrolyte, respectively, has been recently found to result in propagation of accelerated fronts.

ACKNOWLEDGMENTS

We are grateful to A. Alekseev for advice on the theory of operators, and to D. Ruwisch for discussions on active circuits with tunable capacitance. P.R. is indebted to A. Gorbatyuk for the stimulating discussion in the early stages of this work, and acknowledges financial support from the Alexander von Humboldt Foundation.

[1] F. J. Elmer, Phys. Rev. A **41**, 4174 (1990); Z. Phys. B **87**, 377 (1992).
[2] L. Schimansky-Geier, Ch. Zülicke, and E. Schöll, Z. Phys. B **84**, 433 (1991); Physica A **188**, 436 (1992).
[3] F.-J. Niedernostheide, R. Dohmen, H. Willebrand, B. S. Kerner, and H.-G. Purwins, Physica D **69**, 425 (1993).
[4] D. Battogtokh and A. S. Mikhailov, Physica D **90**, 84 (1996).
[5] M. Falcke, H. Engel, and M. Neufeld, Phys. Rev. E **52**, 98 (1995); M. Falcke and H. Engel, *ibid.* **56**, 635 (1997).
[6] *Self-Organization in Activator-Inhibitor-Systems: Semiconductors, Gas Discharge, and Chemical Active Media*, edited by H. Engel, F.-J. Niedernostheide, H. G. Purwins, and E. Schöll (Wissenschaft und Technik Verlag, Berlin, 1996).
[7] I. Schebesch and H. Engel, in *Self-Organization in Activator-Inhibitor-Systems: Semiconductors, Gas Discharge, and Chemical Active Media* (Ref. [6]), p. 120.
[8] F. Mertens, R. Imbihl, and A. Mikhailov, J. Chem. Phys. **101**, 9903 (1994).
[9] F.-J. Niedernostheide, M. Or-Guil, M. Kleinkes, and H.-G. Purwins, Phys. Rev. E **55**, 4107 (1997).
[10] N. Mazouz, G. Flätgen, and K. Krischer, Phys. Rev. E **55**, 2260 (1997).
[11] H. Hempel, I. Schebesch, and L. Schimansky-Geier, Eur. Phys. J. B **2**, 399 (1998).
[12] E. Schöll, *Nonequilibrium Phase Transitions in Semiconductors* (Springer, Berlin, 1987).
[13] A. Alekseev, S. Bose, P. Rodin, and E. Schöll, Phys. Rev. E **57**, 2640 (1998).
[14] A. Wacker and E. Schöll, Z. Phys. B **93**, 431 (1994); S. Bose, A. Wacker, and E. Schöll, Phys. Lett. A **195**, 144 (1994); F.-J. Niedernostheide, H. J. Schulze, S. Bose, A. Wacker, and E. Schöll, Phys. Rev. E **54**, 1253 (1996).
[15] M. Meixner, P. Rodin, and E. Schöll, Phys. Status Solidi B **204**, 493 (1997); Phys. Rev. E **58**, 2796 (1998).
[16] *Proceeding of the International Symposium on Power Semiconductor Devices, Davos, Switzerland, May 31 - June 2, 1994*, edited by W. Fichtner and A. Jaecklin (Swiss Federal Institute of Technology ETH, Zürich, 1994).
[17] D. Ruwisch, M. Bode, H.-J. Schulze and F.-J. Niedernostheide, in *Nonlinear Physics of Complex Systems*, edited by J. Parisi and W. Zimmermann, Lecture Notes in Physics Vol. 476 (Springer, Berlin, 1996), p. 194.
[18] C. Radehaus and H. Willebrand, in *Nonlinear Dynamics and Pattern Formation in Semiconductors and Devices*, edited by F.-J. Niedernostheide (Springer, Berlin, 1995).
[19] A. Gorbatyuk and P. Rodin, Z. Phys. B **104**, 45 (1997).
[20] A. Gorbatyuk and P. Rodin, Solid-State Electron. **35**, 1359 (1992).
[21] E. Ben-Jacob, H. Brand, G. Dee, L. Kramer, and J. S. Langer, Physica D **14**, 348 (1985).
[22] A. S. Mikhailov, *Foundation of Synergetics* (Springer, Berlin, 1994), Vol. 1.
[23] M. Reed and B. Simon, *Methods of Modern Mathematical Physics, Vol. 4.: Analysis of Operators* (Academic Press, New York, 1972).
[24] A. Martin, M. Lerch, P. Simmonds, and L. Eaves, Appl. Phys. Lett. **64**, 1248 (1994).
[25] A. Wacker and E. Schöll, J. Appl. Phys. **78**, 7352 (1995).
[26] D. Ruwisch (private communication).